EUKARYOTIC CELL, Aug. 2007, p. 1400–1410 Vol. 6, No. 8
1535-9778/07/$08.00+0 doi:10.1128/EC.00122-07

Self-Aggregation of *Cryptococcus neoformans* Capsular Glucuronoxylomannan Is Dependent on Divalent Cations▽‡

Leonardo Nimrichter,[1]§ Susana Frases,[2]§ Leonardo P. Cinelli,[3] Nathan B. Viana,[4,5] Antonio Nakouzi,[2] Luiz R. Travassos,[6] Arturo Casadevall,[2,7]†* and Marcio L. Rodrigues[1]†*

Laboratório de Estudos Integrados em Bioquímica Microbiana, Instituto de Microbiologia Professor Paulo de Góes,[1] Instituto de Bioquímica Médica,[3] LPO-COPEA, Instituto de Ciências Biomédicas,[4] and Instituto de Física,[5] Universidade Federal do Rio de Janeiro, 21941-590, Brazil; Department of Microbiology and Immunology[2] and Division of Infectious Diseases of the Department of Medicine,[7] Albert Einstein College of Medicine, 1300 Morris Park Ave., Bronx, New York 10461; and Disciplina de Biologia Celular, Universidade Federal de São Paulo, São Paulo, SP 04023-062, Brazil[6]

Received 13 April 2007/Accepted 1 June 2007

The capsular components of the human pathogen *Cryptococcus neoformans* are transported to the extracellular space and then used for capsule enlargement by distal growth. It is not clear, however, how the glucuronoxylomannan (GXM) fibers are incorporated into the capsule. In the present study, we show that concentration of *C. neoformans* culture supernatants by ultrafiltration results in the formation of highly viscous films containing pure polysaccharide, providing a novel, nondenaturing, and extremely rapid method to isolate extracellular GXM. The weight-averaged molecular mass of GXM in the film, determined using multiangle laser light scattering, was ninefold smaller than that of GXM purified from culture supernatants by differential precipitation with cetyl trimethyl ammonium bromide (CTAB). Polysaccharides obtained either by ultrafiltration or by CTAB-mediated precipitation showed different reactivities with GXM-specific monoclonal antibodies. Viscosity analysis associated with inductively coupled plasma mass spectrometry and measurements of zeta potential in the presence of different ions implied that polysaccharide aggregation was a consequence of the interaction between the carboxyl groups of glucuronic acid and divalent cations. Consistent with this observation, capsule enlargement in living *C. neoformans* cells was influenced by Ca^{2+} in the culture medium. These results suggest that capsular assembly in *C. neoformans* results from divalent cation-mediated self-aggregation of extracellularly accumulated GXM molecules.

Cryptococcus neoformans is a widely distributed microorganism that is the etiologic agent for cryptococcosis, a pulmonary and disseminated mycosis that affects primarily immunosuppressed patients (34). Cryptococcal meningitis and meningoencephalitis may lead to permanent neurological damage, and the mortality rate of patients suffering from cryptococcosis is 12% (http://www.cdc.gov/ncidod/dbmd/diseaseinfo/cryptococcosis_t.htm). Given the high morbidity and mortality associated with cryptococcosis, therapy for this disease remains unsatisfactory, and currently there are no vaccines available to prevent the disease.

C. neoformans is remarkable among eukaryotic pathogenic microbes because of the presence of a polysaccharide capsule composed of galactoxylomannan and glucuronoxylomannan (GXM) (3, 21, 24). Galactoxylomannan has an average mass of 100 kDa, and its biological functions are only beginning to be understood (28, 35). GXM, in contrast, is a 1,700- to 7,000-kDa polysaccharide (28, 29) that comprises up to 90% of the capsule's mass. It consists of an α-1,3-linked mannan main chain with xylosyl and glucuronyl side chains (3, 21, 24). The mannose backbone of GXM is O acetylated, a modification that can influence antibody binding and complement activation (25). Although the biological and structural properties of GXM have been extensively studied, the mechanism by which this polysaccharide contributes to virulence remains poorly understood. There is considerable evidence, however, that GXM interferes with the host immune response by multiple mechanisms (30). Antibodies to GXM are protective (5, 11, 12, 31, 32), and GXM antigens may constitute a potential vaccine against cryptococcosis (9). Moreover, monoclonal antibodies (MAbs) to GXM are in clinical development for patients with cryptococcosis (26).

Recent studies demonstrate that the cryptococcal capsule grows distally by the self-association of GXM fibers (28, 44), but the mechanisms responsible for enlargement remain unclear. Early studies showed that alkaline conditions usually facilitate capsule growth (14, 15, 19, 39, 45), an observation consistent with the view that capsule enlargement occurs when the acidic groups of glucuronic acid (GlcA) residues are ionized. In addition, capsule growth is blocked when *C. neoformans* is cultivated in the presence of high concentrations of sodium chloride (14, 20). Although changes in the ion concentrations of the medium can be expected to have numerous effects on fungal metabolism, these results could suggest that the protonation of the carboxyl groups of GXM or salt formation with monovalent ions results in inhibition of capsule growth.

* Corresponding author. Mailing address for Arturo Casadevall: Department of Microbiology and Immunology, Albert Einstein College of Medicine, 1300 Morris Park Avenue, Bronx, NY 10461. Phone: (718) 430-2215. Fax: (718) 430-8968. E-mail: casadeva@aecom.yu.edu. Mailing address for Marcio L. Rodrigues: Instituto de Microbiologia Professor Paulo de Góes, Universidade Federal do Rio de Janeiro, Centro de Ciencias da Suade (CCS), bloco I, 21941590 Rio de Janeiro, Brazil. Phone: 55 21 2562 6740. Fax: 55 21 2560 8344. E-mail: marcio@micro.ufrj.br.

† A.C. and M.L.R. share senior authorship of this work.

§ L.N. and S.F. contributed equally to this work.

‡ Supplemental material for this article may be found at http://ec.asm.org/.

▽ Published ahead of print on 15 June 2007.

In the present study, we report that concentration by ultrafiltration of cell-free culture supernatant fluids of *C. neoformans* results in the formation of a dense, jellified layer on the filter disc. Chemical, structural, and serological analyses of this viscous film revealed that it consisted of essentially pure GXM, yet it differed in certain physical and immunological properties from GXM prepared by classical precipitation methods. Viscosity analysis suggested that calcium bridges are responsible for the high density of the GXM-containing film. Based on these results, we propose that polysaccharide cross-linking by divalent metals could lead to GXM self-aggregation on the surface of *C. neoformans* and that this process contributes to capsule assembly.

MATERIALS AND METHODS

GXM purification. *C. neoformans* strain ATCC 24067 (serotype D; American Type Culture Collection) was used in all experiments of the current study. *C. neoformans* cells (10^9) were inoculated into 1,000-ml Erlenmeyer flasks containing 400 ml of minimal medium composed of glucose (15 mM), $MgSO_4$ (10 mM), KH_2PO_4 (29.4 mM), glycine (13 mM), and thiamine-HCl (3 μM), pH 5.5. Fungal cells were cultivated for 3 days at 30°C with shaking and separated from culture supernatants by centrifugation at 4,000 × *g* (15 min, 4°C). The supernatant fluids were collected and centrifuged again at 15,000 × *g* (15 min, 4°C) to remove smaller debris. The pellets were discarded, and the resulting supernatant was concentrated approximately 20-fold using an Amicon (Millipore, Danvers, MA) ultrafiltration cell (with a cutoff of 100 kDa and a total capacity of 200 ml) with stirring and Biomax polyethersulfone ultrafiltration discs (63.5 mm) (see Fig. S1 in the supplemental material). A nitrogen (N_2) stream was used as the pressure gas. After the supernatant was concentrated, a thick, translucent film was observed in close association with the ultrafiltration disc and was covered by a concentrated fluid phase. The fluid phase was discarded, and the viscous layer was collected with a cell scraper for storage at room temperature. Fractions that were passed through the 100-kDa filtration discs were filtered through 10-kDa membranes, resulting again in film formation. For polysaccharide quantification, a capture enzyme-linked immunosorbent assay (ELISA) (4), the carbazole reaction for hexuronic acid (10), and the method for hexose detection described by Dubois et al. (13) were used.

NMR analysis. ^{1}H nuclear magnetic resonance (NMR) spectra of de-O-acetylated polysaccharides were recorded using a Bruker DRX 600 apparatus with a triple-resonance probe. The removal of *O*-acetyl groups was performed by dissolving 5 mg of GXM in 1 ml of H_2O, followed by adjustment of the pH to 11.25 with NH_4OH. The resulting solution was stirred for 24 h at 23°C and dialyzed against water (6). Spectra of a de-O-acetylated GXM solution (5 mg in 0.5 ml of 99.9% D_2O; Cambridge Isotope Laboratory) were recorded at 70°C with HOD suppression by presaturation. Homonuclear total correlation spectroscopy (TOCSY) spectra were recorded using states-time proportion phase incrementation for quadrature detection in the indirect dimension. TOCSY spectra were run with 4,096 by 256 points with a spin-lock field of ~10 kHz and a mixing time of 80 ms. Chemical shifts are relative to external trimethylsilylpropionic acid at 0 ppm for ^{1}H. Results obtained in the current analysis were compared with previously described GXM spectral data (1, 2, 6–8).

Monosaccharide analysis. Sugar composition was determined by gas chromatography-mass spectrometry (GC-MS) analysis of the per-*O*-trimethylsilyl (TMS)-derivatized monosaccharides from the polysaccharide film. Methyl glycosides were first prepared from the dry sample (0.3 mg) by methanolysis in methanol-1 M HCl at 80°C (18 to 22 h). The sample was then per-O-trimethylsilylated by treatment with Tri-Sil (Pierce) at 80°C (0.5 h). GC-MS analysis of the per-*O*-TMS derivatives was performed on a model HP 5890 GC interfaced with a model 5970 MSD MS, using a Supelco DB-1 fused-silica capillary column (30 m by 0.25 mm [inside diameter]). The carbohydrate standards used were arabinose, rhamnose, fucose, xylose, glucuronic acid, galacturonic acid, mannose, galactose, glucose, mannitol, dulcitol, and sorbitol.

Binding of divalent metals to GXM. The jellified GXM (2 mg) was diluted to a final volume of 3 ml in 10 mM EDTA and then distributed in dialysis cassettes (molecular mass cutoff, 10 kDa). The GXM-EDTA solution was dialyzed against 1 mM EDTA for 24 h and then against water for 24 h. The resulting solution, considered cation-free GXM, was supplemented with chloride salts of Ca^{2+} or Mg^{2+} to final concentrations ranging from 0 to 10 mM and incubated for 1 h at room temperature. Unbound cations were then removed from the system by ultrafiltration in Millipore concentration tubes (molecular mass cutoff, 100 kDa). The presence of Ca^{2+} or Mg^{2+} in association with the polysaccharide was measured by inductively coupled plasma MS (Quantitative Technologies, Inc., Whitehouse, NJ). A Perkin-Elmer Elan inductively coupled plasma MS was used for metal detection. The elemental content in each sample was determined after comparison with previously constructed calibration curves using cation standards.

Effects of cation binding on the cellular charge of *C. neoformans*. Yeast cells were washed three times with distilled, deionized water and resuspended in 10 mM EDTA. The cell suspension was then dialyzed against 1 mM EDTA for 12 h, with replacement of the chelating solutions by fresh ones after 2-h intervals. The cell suspension was then dialyzed against water by following the same protocol. *C. neoformans* cells were centrifuged and suspended in different solutions of chloride salts of Ca^{2+} and Mg^{2+} and incubated for 2 h. After the removal of unbound ions by washing the cells, zeta potential (ζ) measurements of cellular charge were made using the ZetaPlus zeta potential analyzer (Brookhaven Instruments, Holtsville, NY). ζ is defined as the potential gradient that develops across the interface between a boundary liquid in contact with a solid and the mobile diffuse layer in the body of the liquid. It is derived from the equation $\zeta = (4\pi\eta\eta n)/D$, where D is the dielectric constant of the medium, η is the viscosity, and m is the electrophoretic mobility of the particle.

Viscosity determinations. The characterization of the Brownian motion of polystyrene spheres (radius, 1.52 ± 0.05 μm) immersed in GXM solutions was the parameter used to measure viscosity (40). A water suspension of the spheres (1 μl, 10% [vol/vol]) was dispersed in 150 μl of an extensively dialyzed 0.75-mg/ml solution of GXM. This mixture was placed onto a coverslip with an O ring with a 1-cm diameter and a 0.3-cm width. Alternatively, the GXM solution was supplemented with various concentrations of NaCl (0.01 to 1,000 mM), $CaCl_2$ (0.0001 to 10 mM), or EDTA (0.0001 to 10 mM), or the intact polysaccharide preparation was replaced by an equivalent solution of carboxyl-reduced GXM, prepared according to the method of Taylor and Conrad (38). The O ring was covered with another coverslip to avoid evaporation. The sample was then transferred to an inverted Nikon Eclipse TE300 microscope connected by its epifluorescence port to a neodymium-doped yttrium aluminum garnet laser beam source (with a 1,064-nm wavelength). When the laser beam passes through the objective, it creates an optical trap near the objective focus, allowing the manipulation of small dielectric objects (in order of length measured in micrometers). The microscope was mounted on a Newport table stabilized to avoid vibrations from the environment. The samples were observed with a Plan Apo 100× NA1.4 objective. Digitized images were obtained by a charged-couple-device camera connected to Hamamatsu Argus and Scion frame grabbers. Images were processed using the ImageJ software, elaborated and provided by the National Institutes of Health (http://rsb.info.nih.gov/ij/). The reference distance (height, $h = a$, where h is the distance from the sphere center to the coverslip and a is the bead radius) between the bottom of the coverslip and each sphere was determined by trapping the sphere using the optical tweezers and then moving it towards the coverslip using the microscope knob. After positioning the bead at the desired height, a small image area (50 pixels by 50 pixels) was chosen for frame rate capture (27 to 28 frames per second). The optical tweezers were then alternately turned on and off for periods of 0.5 s by shutting the beam (41).

The mean square displacement of the variation of the image center of mass position δρ in a time interval t is given by:

$$\langle(\delta\rho)^2\rangle = 4Dt \tag{1}$$

where

$$D = \frac{k_B T}{\beta} \tag{2}$$

and β, the Stokes friction coefficient, is a function of the bead radius a and the height h. β is given by the Faxen Law (16):

$$\beta = 6\pi\eta a\left[1 - \frac{9}{16}\left(\frac{a}{h}\right) + \frac{1}{8}\left(\frac{a}{h}\right)^3 - \frac{45}{256}\left(\frac{a}{h}\right)^4 - \frac{1}{16}\left(\frac{a}{h}\right)^5\right]^{-1} \tag{3}$$

For a fixed value of h, $\langle(\beta\rho)^2\rangle$ was calculated, excluding the regions where δρ was <0.01 μm. Those regions correspond to the time intervals for which the bead was trapped. From the linear fit of the measured $\langle(\beta\rho)^2\rangle$ values as a function of time t in equation 1, the diffusion coefficient D was obtained. With the value of D, the Stokes friction coefficient β was determined using equation 2. The sphere height was then changed and the procedure repeated. From the fit of the β values as a function of sphere height h using equation 3, viscosity values were obtained. The described method had 10 to 20% uncertainty for the viscosity determinations.

Effects of exogenously added Ca^{2+} on capsule expression and GXM concentration in culture supernatants. Cryptococci were suspended in a minimal medium similar to that previously described in the text except that $MgSO_4$ was not added. In this medium, containing glucose, KH_2PO_4, glycine, and thiamine-HCl at the concentrations described above and which had a pH of 5.5, cryptococcal growth was similar to that observed in the regular medium (data not shown). After three consecutive passages (at 2-day intervals) into flasks containing the same medium, *C. neoformans* (10^4 yeast cells) was suspended in 100 μl of fresh cation-free medium supplemented with $CaCl_2$ or $MgCl_2$ in concentrations ranging from 0 to 20 mM. After 48 h of cultivation at room temperature in 96-well plates, the cells were recovered by centrifugation for 10 min at 2,000 × *g* and fixed in 2% paraformaldehyde in phosphate-buffered saline (PBS). Supernatants were saved for GXM determination by capture ELISA as previously described (4). The concentration of GXM in culture supernatants obtained from the different growth conditions was normalized to the number of cells in the culture after each condition of stimulation, as measured in a Neubauer chamber. The fixed cells were then washed with PBS, and after they were stained with India ink, the capsule expression was examined microscopically. Capsule sizes, defined as the distances between the outer surfaces of the cell walls and the outer borders of the capsules, were measured by using ImageJ software. All experiments were performed in triplicate sets, and the values were compared using Student's *t* test.

Capsule experiments using dead *C. neoformans* cells. To exclude the possibility that the effects of Ca^{2+} and/or Mg^{2+} on capsule expression were derived from cation regulation of metabolic processes instead of polysaccharide aggregation, the capsule was analyzed in the presence of EDTA and divalent cations using dead cells. *C. neoformans* was killed by heating the cells to 56°C for 1 h, a procedure that results in the killing of 100% of cells (not shown). The dead cells (10^7) were then resuspended in 10 mM EDTA and incubated for 30 min at room temperature, and the capsule sizes were measured as described above. To evaluate whether GXM aggregation and consequent capsule enlargement would occur with dead cells, *C. neoformans* was first exposed to gamma radiation from radioisotope ^{137}Cs to remove external layers of the polysaccharide capsule (27). Briefly, yeast cells (5×10^7) were washed three times and suspended in H_2O to be irradiated for 1 h using the Shepherd Mark I irradiator (JL Shepherd and Associates, San Fernando, CA) at 1,388 rads/min. Polysaccharide release in the supernatant was confirmed by ELISA and India ink staining of irradiated cells (not shown). Irradiated *C. neoformans* cells were then heated as described above and suspended in the divalent cation-free culture medium supplemented with GXM at 100 μg/ml. Calcium chloride was then added to final concentrations ranging from 100 to 0.0001 mM. Yeast suspensions were incubated for 12 h at 30°C, extensively washed with water, and suspended in PBS-bovine serum albumin at 3×10^4 cells/ml. The reactivities of these cells with antibodies to GXM were evaluated by capture ELISA as previously described (4). For this assay, it was assumed that the content of cell-associated GXM was directly proportional to its capture by, and reactivity with, antibodies to GXM. Relative values of GXM expression were obtained by dividing the ELISA absorbance values after incubation of the yeast cells with GXM by those obtained immediately after irradiation, which are considered the basal levels of polysaccharide expression.

Molecular mass determination of GXM. Molecular masses were calculated by multiangle laser light scattering by following the conditions described by McFadden et al. (29). The polysaccharides obtained were diluted in sterile-filtered, degassed, ultrapure water to the desired concentrations from a freshly made 5-mg/ml stock solution. GXM samples included preparations obtained by ultrafiltration as well as by cetyl trimethyl ammonium bromide (CTAB) precipitation (8). To evaluate whether stirring would have any effect on the molecular mass, a 1-mg/ml solution of CTAB-precipitated polysaccharide was stirred with a magnetic bar for 24 h for further measurement of molecular mass. The change in the refractive index (*dn*/*dc*) of the samples was measured by differential refractometry using a 620-nm laser source (BI-DNDC; Brookhaven Instruments Corp., Holtsville, NY) at 30°C. The molecular mass was determined at room temperature by multiangle laser light scattering (using a BI-MwA analyzer; Brookhaven Instruments Corp., Holtsville, NY) using a 675-nm laser source. Before the mass measurements were taken, the system was calibrated against toluene and normalized for Rayleigh scattering with 20-nm microspheres (Duke Scientific Corp., Palo Alto, CA). The weight-averaged mass (M_w) was calculated by the Zimm equation (46), $Kc/\Delta R(\theta) = 1/(M_w)[P(\theta)] + 2A_{2c}$, where K is the optical constant, defined as the quotient of $4\pi^2 n_o^2 (dn/dc)^2 / N_A \lambda_o^4$, and $\Delta R(\theta)$ is the excess Rayleigh factor, determined by comparing the sample and solvent values at angle (θ) and concentration (c). $P(\theta)$ is the particle scattering function, A_2 is the second virial coefficient, n_o is the refractive index of the solvent, N_A is Avogadro's number, and λ_o is the modal wavelength of the laser source. The *dn*/*dc* values were adjusted according to the Cauchy equation, $dn/dc = A + B/\lambda^2$, using a B coefficient for aqueous solutions of +0.0022 μm and wavelengths (λ) in micrometers to accommodate the longer wavelength of the molecular weight analyzer. Depolarization corrections were assumed to be negligible. All samples were passed through an in-line 0.8-μm syringe filter to eliminate large aggregates and reduce extraneous sources of refracted or scattered light.

TABLE 1. Average molecular masses, radius of gyration (R_g) values, and mass density (M_w/R_g) values of GXM

GXM derivation method	M_w (g/mol)	R_g (nm)	M_w/R_g (10^3)
CTAB precipitation[a]			
Standard conditions	2.2×10^6	88.6	24.83
With stirring	1.8×10^6	79.4	22.6
Ultrafiltration	2.4×10^5	141.0	1.74

[a] As described by Cherniak et al. (8). CTAB-derived GXM samples were analyzed under standard conditions or after 24 h of stirring.

Binding of MAbs to GXM. Binding of MAbs to GXM obtained by precipitation with CTAB (8) or by the current ultrafiltration methodology was evaluated by ELISA (4) and dot blot analysis. For the ELISA, polysaccharide solutions at 5 nM, calculated from the data presented in Table 1, were used to coat the wells of 96-well plates. GXM detection was performed using two immunoglobulin M (IgM) MAbs, known as 12A1 and 21D2 (33), and an IgG1, known as 18B7 (5). Reactions were developed after the incubation of the plates with alkaline phosphatase-conjugated goat anti-mouse IgM or IgG1 followed by the addition of *p*-nitrophenyl phosphate and measured at 405 nm with a Multiscan MS (Labsystem, Helsinki, Finland). For the dot blot analysis, 0.5 nmol GXM in 2 μl water was loaded onto nitrocellulose membranes. The membranes were allowed to dry for 1 h at 37°C and then were blocked with PBS containing 1% bovine serum albumin. Blocked membranes were incubated with the antibodies described above at starting dilutions of 10 μg/ml. After being washed extensively, membranes were sequentially incubated with alkaline phosphatase-conjugated goat anti-mouse IgM or IgG1 and *p*-nitrophenyl phosphate solutions. Reactions were quantified by the transfer of the soluble, colored products to the wells of 96-well plates and reading at 405 nm as described above.

RESULTS

Extracellular GXM aggregates to form a highly viscous film. After the complete removal of cells and debris by centrifugation, *C. neoformans* supernatants (at initial volumes of 800 ml) were concentrated in ultrafiltration cells. Final volumes of 40 ml were achieved, and the upper fluid phase was removed. Sticky, translucent, 2- to 4-mm-thick films were obtained on the surfaces of the ultrafiltration discs (see Movie S1 in the supplemental material). Concentration rates of supernatants from different cultures varied, but films were always formed after 1 to 3 h of ultrafiltration. The viscous films were then collected with a cell scrapper and stored at room temperature for further analysis. The final volume of the viscous film preparation obtained from 800-ml cultures ranged from 10 to 15 ml. Interestingly, film formation was also observed when supernatant fractions that were passed through the 100-kDa membrane were concentrated using 10-kDa filtering discs (data not shown). Serotype A *C. neoformans* strains and *Cryptococcus gattii* isolates (serotypes B and C) were used under the same conditions, with similar results being obtained (data not shown).

Based on the high concentrations of GXM in cryptococcal supernatants and its known ability to self-aggregate (29), we suspected that the viscous film observed in the concentration system could contain capsular polysaccharide shed into the culture medium during fungal growth. The concentration of GXM in this material was 7.5 mg/ml as measured by capture ELISA.

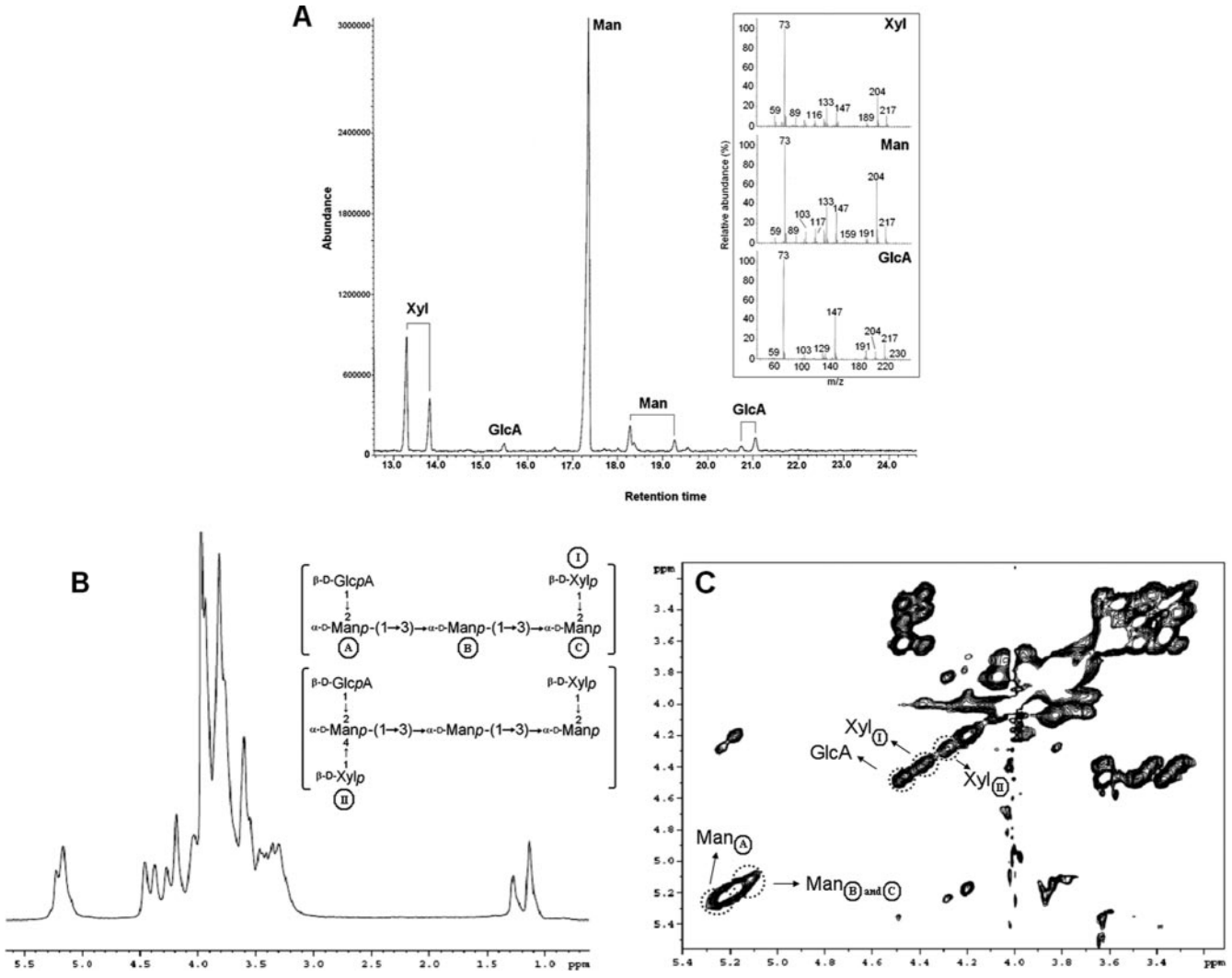

FIG. 1. Structural analysis of the cryptococcal polysaccharide isolated by ultrafiltration. (A) GC-MS analysis revealed peaks with retention times similar to those observed using standards of the typical GXM components (Man, Xyl, and GlcA). The inset shows a fragmentation profile of the most abundant peak for each sugar detected by MS. (B) ^{1}H NMR spectrum of the de-O-acetylated molecule and, in the inset, the identified polysaccharide components in the current analysis. (C) TOCSY spectrum of the de-O-deacetylated structure. Regions corresponding to the sugar units shown in panel B were assigned as shown.

After acidic methanolysis of the sample, monosaccharide constituents were analyzed by GC (Fig. 1A). This analysis allows the potential detection of four different peaks for each sugar derivative, corresponding to the α and β forms of furanose and pyranose rings. In association with MS analysis, each peak could be precisely identified based on the profile of the fragmentation observed. The fragmentation of TMS derivatives of hexoses usually generates diagnostic peaks at *m*/*z* 217 and 214 (23). Pyranose rings give rise to a (*m*/*z* 204)/(*m*/*z* 217) ratio of >1, whereas furanose rings show a ratio of <1.

Peaks with retention times corresponding to standard derivatives of the typical GXM components mannose (Man), xylose (Xyl), and GlcA were detected (Fig. 1A). Three Man peaks were observed at retention times of 17.3 min (90%, relative intensity), 18.2 min (8%, relative intensity), and 19.3 min (2%, relative intensity). By MS, these peaks were identified, respectively, as α-pyranosyl, β-pyranosyl, and furanosyl forms of TMS-Man (22). The peaks with retention times of 13.3 min (67%, relative intensity) and 13.8 min (33%, relative intensity) were characterized as α- and β-pyranosyl forms of Xyl. Finally, the minor peaks with retention times of 15.5, 20.8, and 21.0 min corresponded to the different anomers of the TMS derivatives of GlcA. The profile of fragmentation of the major peak of each sugar is shown in the inset to Fig. 1A.

Man was the major polysaccharide constituent (59.4% of the molar mass), followed by Xyl (32.1%) and GlcA (8.5%). These results strongly indicate that the film deposited on the filtration disc consisted of GXM. Rhamnose, fucose, glucose, mannitol, and galactose were not detected in the samples analyzed by GC-MS. The high carbohydrate content together with the monosaccharide analysis suggests that the film deposited on the filtration disc was composed largely, if not exclusively, of GXM. This information was supported by the lack of protein detection by colorimetric and electrophoretic methods (data not shown).

The purity and fine structure of the polysaccharide were further confirmed by NMR analysis. Based on previous reports on the structure of GXM (2, 7), structural reporter groups and branches have been identified. The reference structures were the pentasaccharide and the hexasaccharide, shown in Fig. 1B and 1C, described as the most frequent repeating units in isolate B-3501, a serotype D strain, and in Cap70, a capsule-deficient mutant of this strain (2). The one-dimensional ^{1}H spectrum of the de-O-acetylated polysaccharide had signals at 5.21 ppm, assigned to Man H-1 (residue A), and 5.15 ppm, representing the combined H-l chemical shifts of Man residues B and C. The peaks observed at 4.45 and 4.35 ppm were assigned to H-1 resonances of GlcA and Xyl (residue I), respectively. The signal detected at 4.25 ppm corresponds to H-1 of Xyl II. These chemical shifts are all characteristic of serotype D GXM (2, 7). The double-quantum-filtered TOCSY spectrum was interpreted using the information obtained in the ^{1}H spectrum and from previous studies (1, 2, 6–8). The chemical shifts of the cross peaks labeled in Fig. 1C are consistent with those H-1 assignments observed for the three mannosyl residues (A, B, and C), GlcA residues, and Xyl residues (I and II). Complete chemical shift assignments for Man, Xyl, and GlcA residues of the presently analyzed polysaccharide were compared with those described previously for GXMs (1, 2, 6–8), confirming that the currently characterized molecule represents the serotype D polysaccharide.

GXM aggregation is mediated by divalent ions. Anionic polysaccharide chains can cross-link through bridges formed by the interaction of divalent ions with the anionic sugar units (42). We therefore hypothesized that the formation of GXM aggregates after supernatant filtration depended on the interaction of negatively charged GlcA residues and divalent metals, which are abundant in the culture medium as Mg^{2+} salts. Our premise was that two GlcA residues from different GXM chains could interact with one atom of the divalent ion, generating cross-linked polysaccharide chains. In this case, the formation of cross-linkages would not take place if negative charges were not abundant or if monovalent ions as well as chelators of divalent cations were present in high concentrations.

First, we analyzed the ability of GXM to bind to the divalent cations Mg^{2+} and Ca^{2+}. A cation-free solution of the GXM film was incubated in the presence of various concentrations of Ca^{2+} and Mg^{2+} chloride salts. As demonstrated in Fig. 2A, a dose-dependent binding of these metals to the polysaccharide was observed. Metal binding to surface-associated GXM was observed using intact *C. neoformans* cells (Fig. 2B). A dose-dependent decrease of cellular charge was observed when *C. neoformans* was treated with chloride salts of Mg^{2+} and Ca^{2+}, supporting the hypothesis that divalent metals bind to the negatively charged polysaccharide.

The results depicted in Fig. 2 were in agreement with the hypothesis that, as demonstrated with plant polysaccharides (42), the high viscosity observed with the GXM film is a consequence of the interaction of negatively charged GlcA units in the GXM with divalent cations. Consequently, we analyzed the influence of the negative charges of GlcA on the viscosity of the thick material obtained by ultrafiltration. After the carboxyl reduction of the polysaccharide, approximately 95% of the total content of GlcA was converted to glucose, as determined spectrophotometrically. The viscosity of the reduced polysaccharide solution fell to approximately 10% of that of the native GXM film (Fig. 3A). This result implied that the presence of the negative charges in the GlcA residues was necessary for polysaccharide aggregation.

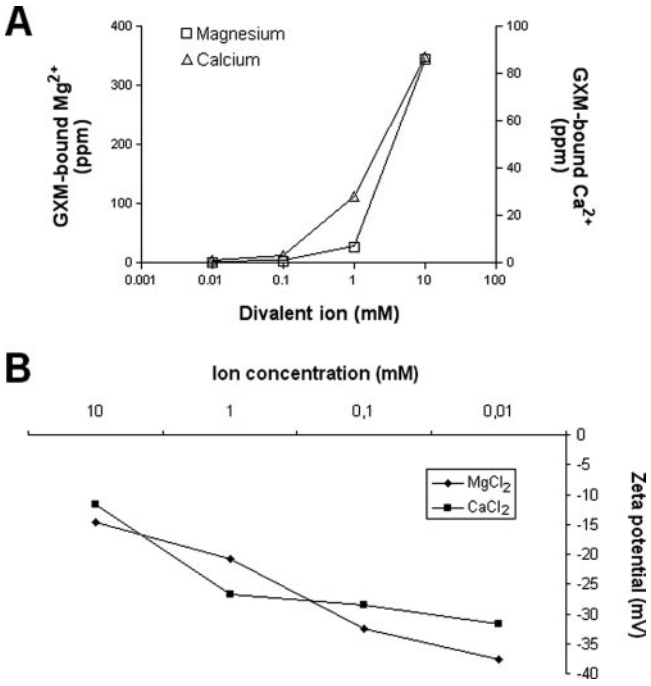

FIG. 2. Ca^{2+} and Mg^{2+} binds to GXM and affects cellular charge. (A) A cation-free preparation of GXM was treated with various concentrations of the divalent ions, and after the removal of unbound elements, the Ca^{2+} and Mg^{2+} content was determined. A dose-dependent profile of binding to GXM was observed for each metal. (B) After the removal of divalent ions by treatment with EDTA and extensive dialysis, the cellular charge of *C. neoformans* was measured in a zeta potential analyzer. An inverse relationship between negative charge and metal binding was observed.

We therefore analyzed the influence of different concentrations of Na^+ and EDTA on the viscosity of the GXM film obtained by ultrafiltration. Na^+ caused a dose-dependent decrease in the viscosity of a polysaccharide solution at 0.75 mg/ml, as shown in Fig. 3B. Similar results were observed when the polysaccharide was treated with EDTA (Fig. 3C). Significant differences ($P < 0.01$, Student's t test) were observed between viscosity values obtained in the absence of Na^+ or EDTA and those obtained after incubation of the polysaccharide with the highest concentration of each compound. We then evaluated whether the viscosity of GXM would be affected by treatment with $CaCl_2$. The results shown in Fig. 3D demonstrate that Ca^{2+} concentrations lower than 0.1 mM were associated with increased polysaccharide viscosity. Higher concentrations, however, resulted in decreased levels of viscosity, indicating that the stoichiometry of the association between Ca^{2+} and GlcA residues shifted from the bridge-forming ratio of 1:2 to 1:1, with a subsequent decrease in the efficacy of association between different GXM fibers. Based on the results obtained with the GC-MS analysis, the concentration of GlcA in the 0.75-mg/ml solution of GXM was estimated to be approximately 0.4 mM. Consequently, Ca^{2+} concentra-

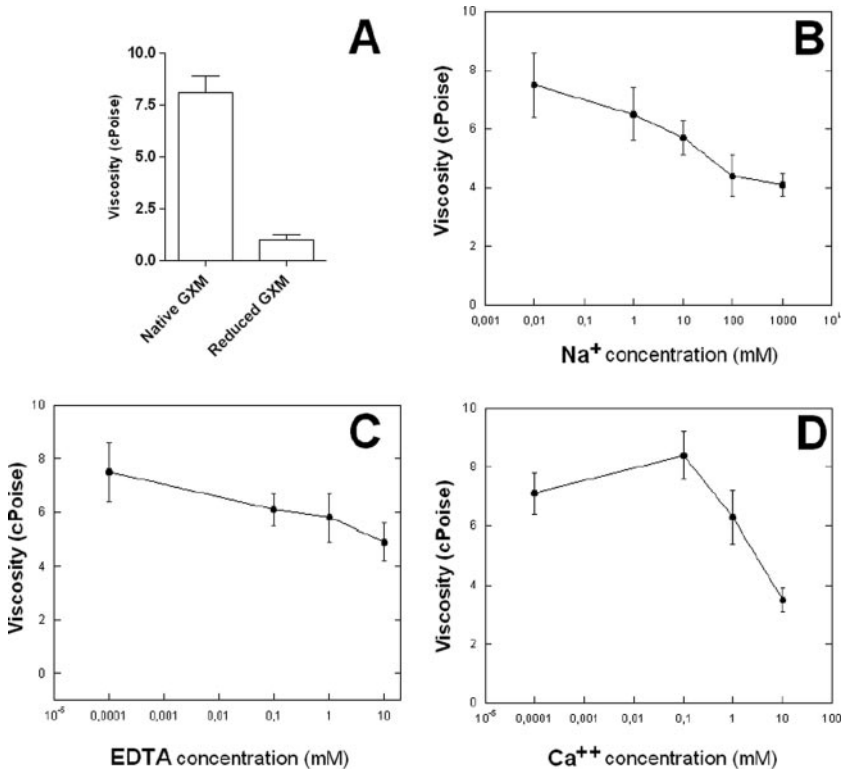

FIG. 3. Influence of GlcA negative charges (A), a monovalent cation (B), a chelating agent (C), and a divalent cation (D) on the viscosity of isolated GXM. (A) A reduction of around 95% of the content of GlcA in GXM was associated with a 90% decrease in polysaccharide viscosity ($P < 0.05$). Viscosity decreased in a dose-dependent way when Na^+ (B) and EDTA (C) were used. Low Ca^{2+} concentrations induced an increase in polysaccharide viscosity, which was reversed with large amounts of the divalent ion (D). Results are means of three different measurements ± standard deviations.

tions higher than 0.2 mM should exceed the 1:2 Ca^{2+}/GlcA molar ratio. In fact, Ca^{2+} concentrations in the range of 1 to 10 mM caused a marked decrease in polysaccharide viscosity. These results indicate that the availability of Ca^{2+} can regulate GXM aggregation. When Ca^{2+} was replaced by Mg^{2+}, similar results were obtained (data not shown).

Capsule growth is influenced by divalent metals. The results shown in Fig. 2 and 3 led us to investigate whether divalent cations would influence capsule enlargement in *C. neoformans*. Different assays using EDTA to chelate ions or divalent cations to regulate capsule expression were performed. Ca^{2+} and Mg^{2+} at 0 to 20 mM were used under the same conditions, with similar results being obtained. The results described below correspond to the experimental procedures using Ca^{2+}.

EDTA-treated dead *C. neoformans* cells had an average capsule size smaller than that observed for untreated dead cells (Fig. 4A). Divalent ions appeared to be relevant for capsule assembly; differences in the average capsule size were observed when *C. neoformans* was cultivated with various concentrations of Ca^{2+} (Fig. 4B). Yeast cells grown in the absence of divalent ions had smaller capsules, although the concentration of GXM was higher in supernatants than under any other culture condition, a finding consistent with the reduced ability of *C. neoformans* to retain polysaccharides in the capsule. The addition of increasing concentrations of Ca^{2+} to the culture medium resulted in augmented capsule expression associated with decreased levels of soluble GXM in fungal cultures. Very large capsules were observed in yeast cells cultivated in the range of 0.01 to 0.3 mM Ca^{2+}. However, similarly to what has been observed in the viscosity assays, high concentrations of $CaCl_2$ caused a decrease in capsule sizes.

Although the results described above strongly support the proposal that divalent cation-mediated aggregation of GXM is involved in capsule enlargement, the possibility that the regulation of gene expression and/or enzymatic activity was influenced by capsule synthesis could not be excluded. We therefore examined the ability of poorly encapsulated dead cells of *C. neoformans* to incorporate exogenously added GXM in the presence of various Ca^{2+} concentrations. To enhance the detection of newly incorporated GXM chains, *C. neoformans* cells were first irradiated to remove the existing external polysaccharide layers. GXM incorporation was then evaluated by the quantitative reactivity of yeast cells with antibodies to the polysaccharide (4). The binding of GXM to dead cells was directly influenced by the availability of calcium (Fig. 4D). This result indicates that, even in the absence of an active cellular metabolism, GXM fibers can aggregate to the cell surface of *C. neoformans* in a process modulated by divalent cations.

Comparison of GXM molecules obtained by ultrafiltration and CTAB precipitation. The average molecular masses of GXM obtained in the ultrafiltration cell or CTAB precipitation (Table 1) were determined as described by McFadden and coworkers (29). The molecular mass of the CTAB-derived polysaccharide was comparable to that described previously for

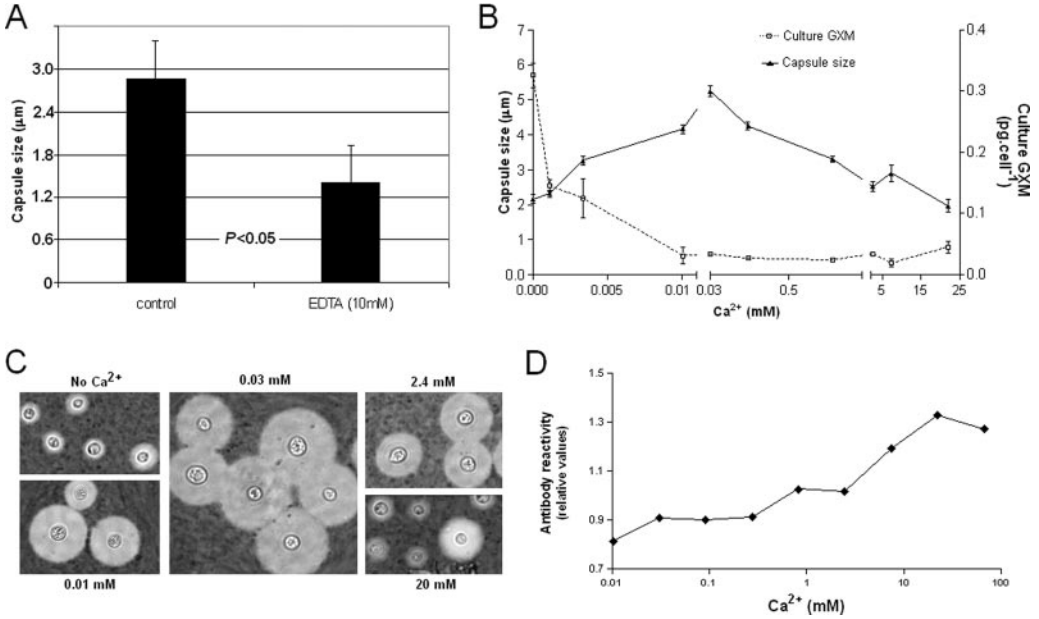

FIG. 4. Influence of divalent ions on capsule expression. (A) Treatment of dead yeast cells with EDTA resulted in a significantly reduced capsule size. (B) Increasing concentrations of Ca^{2+} initially induce an enhancement in capsule expression, but excess cation concentrations cause a decrease in capsule size. (C) Images of the most-representative capsule size-related events shown in panel B are depicted, with emphasis on the very large capsules observed after fungal cultivation in the presence of 0.03 mM $CaCl_2$. (D) The incubation of dead, poorly encapsulated *C. neoformans* cells with GXM in the presence of various Ca^{2+} concentrations results in polysaccharide incorporation, as determined by capture ELISA (4).

serotype D GXM (29). However, the average mass of the polysaccharide purified by filtration was ninefold smaller. The lower molecular mass observed for the filtered GXM was not a consequence of mechanical shearing due to stirring, since the CTAB-derived polysaccharide incubated for 24 h with stirring had a molecular mass similar to that detected under regular conditions. Other structural aspects were also determined based on the light scattering data. Polysaccharide molecules obtained by ultrafiltration had higher radius of gyration values. This parameter was used in conjunction with M_w to calculate the mass density of GXM from each preparation, revealing that CTAB-derived polysaccharides were about 14-fold more dense than filtered molecules. Interestingly, treatment of the filtered polysaccharide with CTAB generated molecular weight measurements similar to those obtained for the CTAB-derived GXM, consistent with the notion that CTAB aggregates GXM (S. Frases and A. Casadevall, unpublished results).

The data presented above suggested that GXM molecules obtained from ultrafiltration cells are structurally different from those purified by detergent precipitation. Since structural features are directly related to antigenic properties, we evaluated the reactivities of polysaccharides obtained by both methods with MAbs using an ELISA and a dot blotting assay. Three different GXM-binding MAbs that bind different epitopes were used for the antigenic analysis: 12A1, 18B7, and 21D2. As shown in Fig. 5, GXM obtained by filtration and the polysaccharide precipitated with CTAB were similarly recognized by MAb 21D2. However, the filtered polysaccharide reacted more strongly with MAbs 12A1 and 18B7 than CTAB-precipitated GXM did, suggesting differences in epitope prevalence and/or accessibility.

DISCUSSION

Synthesis and assembly of capsular components are key events in the biology of *C. neoformans*. Several reports indicate that capsule expression and/or enlargement in *C. neoformans* is probably a multifactorial biological event controlled at different levels (21, 22, 24, 28, 29, 37, 43–45). For instance, it has been reported recently that *CIR1*, a gene identified as a *Cryptococcus* iron regulator, controls the expression of all known virulence factors, including capsule, melanin, and growth at host temperature (22). In addition, capsule expression in *C. neoformans* apparently requires the transport of the polysaccharide to the extracellular environment in Golgi body-derived vesicles that traverse the cell wall and, presumably, release capsular components by a yet undetermined mechanism (37, 43). Capsule assembly at the extracellular face of the cell wall involves the production of GXM fibers that include both attached and released forms (29). The analysis of capsule growth using complement as a marker of the old capsule revealed that the old capsular material remains close to the cell wall during capsular enlargement (44). The mechanisms by which GXM fibers self-aggregate during apical capsule growth were still unclear, however.

In the present work, we report the serendipitous observation that the ultrafiltration and concentration of *C. neoformans* supernatants resulted in the formation of a jellified polysaccharide film that allows the use of a one-step procedure for the isolation of capsular polysaccharide. Most importantly, this finding also provided a new insight into the mechanisms of capsule assembly that, together with well-described mechanisms of GXM synthesis and secretion (21, 24, 28, 29, 37, 43)

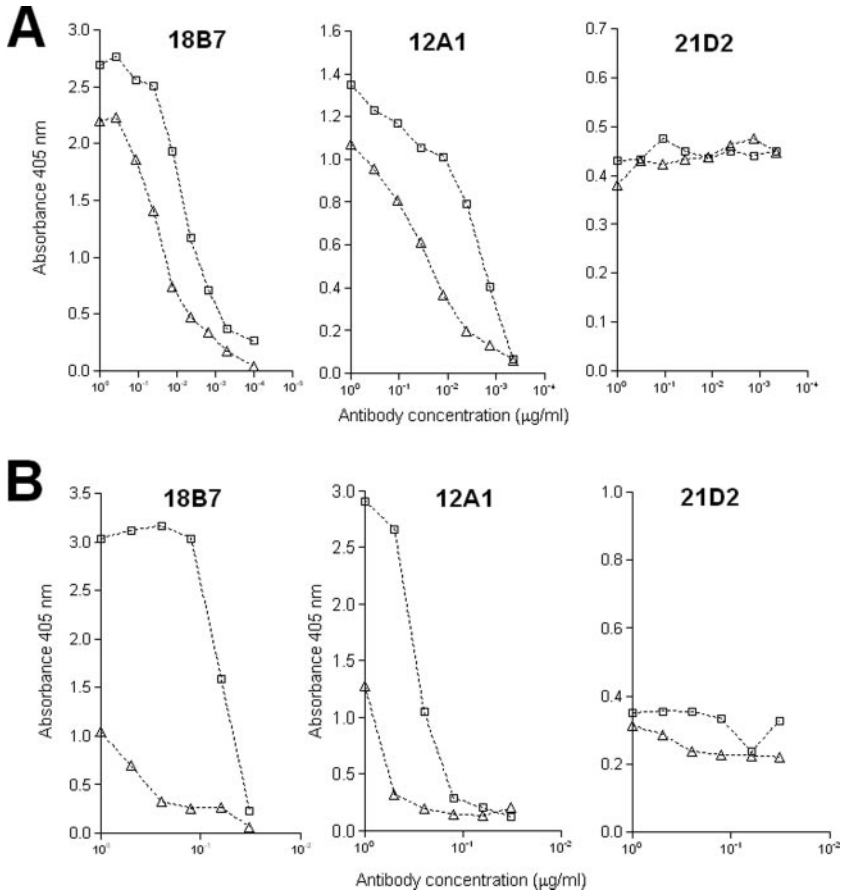

FIG. 5. Binding of MAbs to GXM obtained by CTAB precipitation (triangles) and ultrafiltration (squares) as determined by ELISA (A) and dot blot analysis (B). Different MAbs were used for the reactions with the polysaccharides, including 18B7, 12A1, and 21D2. Polysaccharide samples included GXM obtained by ultrafiltration and CTAB precipitation.

and other still unknown steps of polysaccharide self-association, illustrate how the cryptococcal capsule enlarges.

Our finding that GXM coalesced into a polysaccharide film, or gel, under conditions of flow-directed, increased concentration indicates that the molecule is capable of self-aggregation and that this phenomenon is dependent on polysaccharide concentration and perhaps directional flow. Both flow and concentration are likely to be relevant parameters for *C. neoformans* capsule assembly, since capsule density varies as a function of radial position and apical growth requires GXM transport to the capsule edge from intracellular sites of biosynthesis. The fact that film formation was also observed when supernatant fractions with molecular masses smaller than 100 kDa were filtered through 10-kDa membranes confirms the high diversity in the molecular masses of GXM molecules (29) and indicates that polysaccharide aggregation does not depend on molecular weight.

To investigate mechanisms that could contribute to self-aggregation, we studied the effect of divalent cations on GXM viscosity. These ions are abundant in the culture medium (Mg^{2+}) used in the present study, which led us to hypothesize that cross-linking between GXM fibers would require a divalent metal ion for two different GlcA residues. The efficacy of this association would depend on water removal and increased polysaccharide concentration, which should allow an efficient interaction between GXM fibers and divalent ions at neutral and alkaline pHs (pK of glucuronides, $\geq$3). Accordingly, the carboxyl reduction of GXM film, as well as its treatment with EDTA, monovalent ions, and excessive concentrations of Ca^{2+}, reduced viscosity, supporting the role of divalent metals on GXM aggregation. The direct interaction of polysaccharide chains with divalent ions was also demonstrated, as inferred from the reduced cellular charge of Mg^{2+}- and Ca^{2+}-treated cryptococci and direct binding of the cations to GXM.

Early studies suggested that cultivation of *C. neoformans* in high concentrations of NaCl (1 M) was associated with inhibition of capsule growth. Since this effect does not generally apply to other solutes (20), we assumed that capsule growth could be inhibited in the presence of Na^{+} by the univalent neutralization of negatively charged GlcA residues. In this case, divalent ions would be expected to positively modulate capsule assembly in concentrations compatible with the 1:2 metal/GlcA ratio and reduce the capsule when provided in excess. We therefore cultivated *C. neoformans* with various concentrations of Ca^{2+} and determined the capsule size. In agreement with the viscosity assays, low concentrations of Ca^{2+} stimulated capsule growth, and higher concentrations inhibited capsule assembly. At the higher Ca^{2+} concentrations,

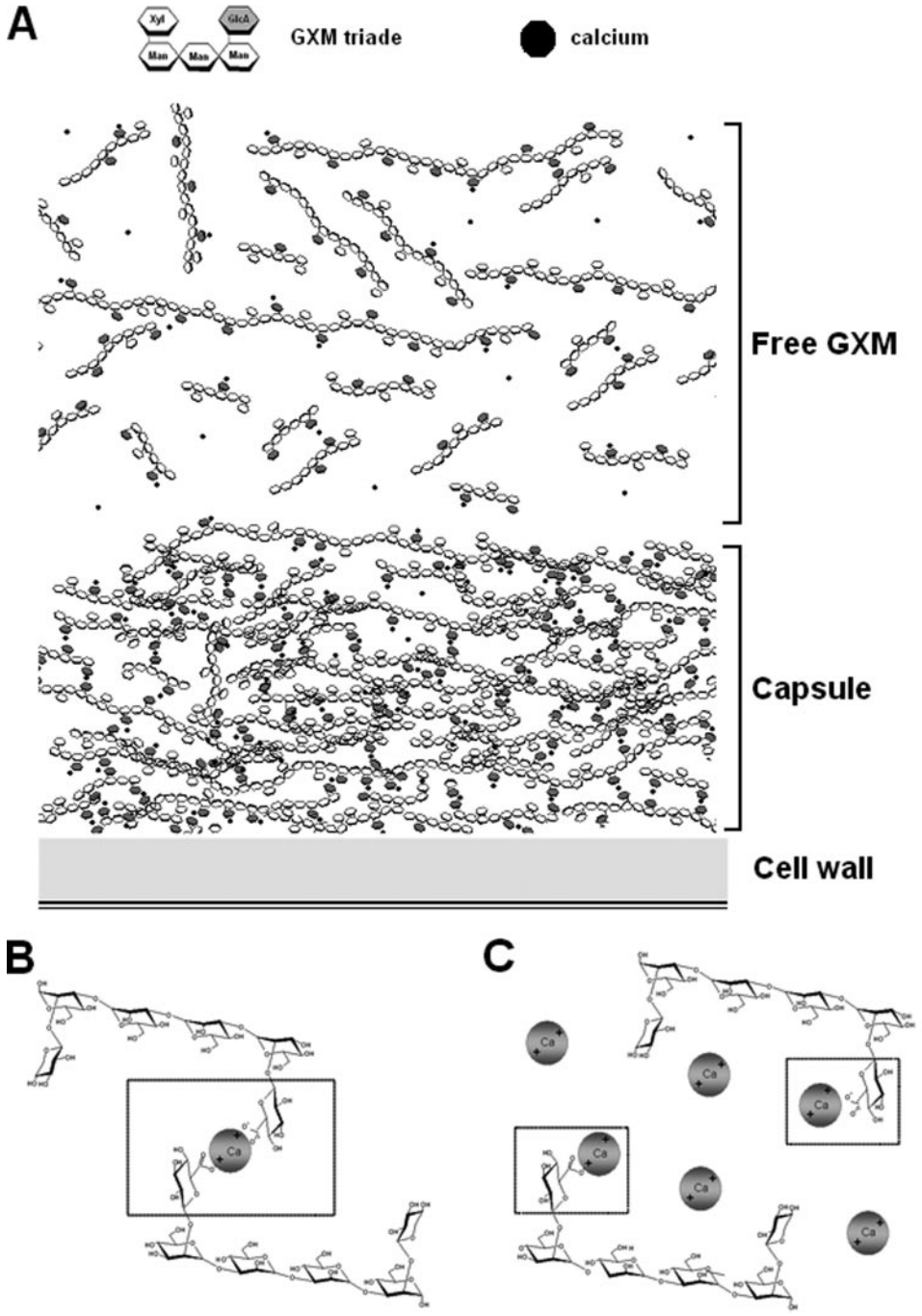

FIG. 6. Proposed model for GXM assembly on fungal cell surface. (A) GXM polymers are first covalently attached to the cell wall (not shown). Extracellular GXM chains (Free GXM) are then layered by metal-mediated cross-linking. Each atom of Ca^{2+} makes salt bridges between two GlcA residues that are frequently from different polysaccharide fibers. (B) Binding of divalent ions to GlcA residues at a 1:2 ratio would support capsule growth. (C) Excessive concentrations would neutralize GlcA negative charges, precluding capsule enlargement.

saturation of GlcA residues by univalent calcium binding would be expected to preclude intermolecular bridge formation. A model proposing the influence of divalent ions on the growth of the cryptococcal capsule is shown in Fig. 6. This model is supported by the fact that in plant cell walls, pectin galacturonans can be cross-linked by the insertion of Ca^{2+} ions between the unesterified carboxyl groups of the galacturonosyl residues (42).

Capsule expression is regulated during *C. neoformans* infection. For example, the capsule of yeast cells harvested from infected tissues showed a greater matrix density than yeast cells grown in vitro under capsule induction conditions (18). Capsule expression varies according to the organ colonized by cryptococci (17, 36), which may have a relationship with the tissue concentration of divalent metals and perhaps pH, since tissue pH would affect the ionization of GlcA carboxyl groups.

This observation may be directly associated with the resistance of *C. neoformans* to host defenses given that the primary function of the polysaccharide is to avoid phagocytosis (25, 30). On the other hand, GXM release by *C. neoformans* could also influence the availability of key regulators of physiological processes such as Ca^{2+} and Mg^{2+}. Since divalent metals can be sequestered in the GXM fibers, their effective physiological concentrations could be reduced in the presence of excess polysaccharide.

Methods for the purification and structural analysis of GXM have been intensively studied (1, 2, 6–8). Classical techniques of polysaccharide purification include precipitation with ethanol and recovery of anionic structures by precipitation with cationic detergents (8). It remains unclear, however, how the reagents used in the different steps of GXM purification influence the polysaccharide structure. Furthermore, cationic detergents are notoriously difficult to remove from GXM preparations, and there is always the concern that such impurities may contribute to the biological properties attributed to GXM. Our findings revealed that the concentration of cryptococcal supernatants in ultrafiltration cells resulted in the deposition of a dense and viscous layer over the filtration disc. Spectrometric and sugar compositional analyses revealed that this jellified preparation consisted of essentially pure GXM. Such a fast and efficient method of GXM isolation involves no denaturing treatment or chemical modification of the polysaccharide. The fact that GXM alone was found in the purified preparation agrees with the fact that negative charges in polysaccharides are determinants of molecular aggregation.

The molecular masses, lengths, and antigenicities of GXM obtained by ultrafiltration and CTAB precipitation differed considerably. Two of the MAbs used, 12A1 and 18B7, reacted more intensely with the preparation obtained by concentration in the ultrafiltration cell than with CTAB-derived GXM. In contrast, the reactivities of both polysaccharide preparations with MAb 21D2 were similar. We note with interest that our NMR analysis of ultrafiltered GXM indicated the presence of a mannosyl triad whose presence has been described previously only for a mutant strain of *C. neoformans* (2). This triad is not one of the six classical triads described by Cherniak and collaborators for serotype D GXM (7), and its presence is consistent with structural differences that may translate into antigenic differences. The molecular weight of EDTA-treated polysaccharide was also analyzed, although no reduction in molecular weight was observed (data not shown). Such information, together with the fact that the removal of Ca^{2+} by EDTA treatment loosened some, but not all, polysaccharide (Fig. 4A), indicates not only that the cation contributes to capsule assembly but also that other molecular forces are operative in holding the capsular polysaccharide together.

The finding that ultrafiltration-derived GXM had an average mass that was ninefold smaller than that of CTAB-derived GXM could have important biological implications. At the very least, this observation suggests that there are many more molecules of GXM on a mass basis than had been assumed. Smaller-molecular-mass GXM can be expected to have different pharmacokinetic and tissue penetration properties than larger-molecular-mass GXM. The larger molecular mass of CTAB-purified GXM presumably reflects the preferential precipitation of larger molecules or detergent-mediated aggregation. Given that most biological studies of the effects of GXM on host immunity have been carried out with CTAB-purified GXM, it is possible that these findings represent effects associated only with the large GXM complexes. Hence, the method described here provides the means to recover a fraction of GXM that was previously unsuspected. The challenge ahead is to understand how larger and smaller GXM fibrils are assembled into a polysaccharide capsule. The observation that self-aggregation of GXM fibers is mediated by divalent cations suggests that much of the information required for capsule assembly may be found within the structure of GXM itself, which appears to have the capacity to self-assemble in complex intermolecular lattices.

ACKNOWLEDGMENTS

We are indebted to Ronald Schnaar for his critical reading of the manuscript, Ana Paula Valente for help with the use of NMR equipment, Leonardo Tavares for helpful suggestions, Diane McFadden for help with light scattering analysis, and Fernanda L. Fonseca for help with the movie in the supplemental material.

The present work was supported by Coordenação de Aperfeiçoamento de Pessoal de Nível Superior (CAPES, Brazil), Conselho Nacional de Desenvolvimento Científico e Tecnológico (CNPq, Brazil), Instituto do Milênio de Nanociências, Instituto do Milênio de Avanço Global e Integrado da Matemática Brasileira, and Fundação de Amparo a Pesquisa do Estado do Rio de Janeiro (FAPERJ, Brazil). M.L.R. was the recipient of an International Fellowship for Latin America (2005), provided by the American Society for Microbiology. L.R.T., L.N., and M.L.R. are recipients of career research fellowships from CNPq. A.C. is supported by NIH grants AI033142, AI033774, AI052733, and HL059842. Carbohydrate analyses were performed at the Complex Carbohydrate Research Center, University of Georgia (Atlanta), which is supported in part by the Department of Energy-funded Center for Plant and Microbial Complex Carbohydrates (DE-FG-9-93ER-20097).

REFERENCES

1. **Bacon, B. E., and R. Cherniak.** 1995. Structure of the *O*-deacetylated glucuronoxylomannan from *Cryptococcus neoformans* serotype C as determined by 2D 1H NMR spectroscopy. Carbohydr. Res. **276:**365–386.
2. **Bacon, B. E., R. Cherniak, J. Kwon-Chung, and E. S. Jacobson.** 1996. Structure of the O-deacetylated glucuronoxylomannan from *Cryptococcus neoformans* Cap70 as determined by 2D NMR spectroscopy. Carbohydr. Res. **283:**95–110.
3. **Bose, I., A. J. Reese, J. J. Ory, G. Janbon, and T. L. Doering.** 2003. A yeast under cover: the capsule of *Cryptococcus neoformans*. Eukaryot. Cell **2:**655–663.
4. **Casadevall, A., J. Mukherjee, and M. D. Scharff.** 1992. Monoclonal antibody based ELISAs for cryptococcal polysaccharide. J. Immunol. Methods **154:** 27–35.
5. **Casadevall, A., W. Cleare, M. Feldmesser, A. Glatman-Freedman, D. L. Goldman, T. R. Kozel, N. Lendvai, J. Mukherjee, L.-A. Pirofski, J. Rivera, A. L. Rosas, M. D. Scharff, P. Valadon, K. Westin, and Z. Zhong.** 1998. Characterization of a murine monoclonal antibody to *Cryptococcus neoformans* polysaccharide that is a candidate for human therapeutic studies. Antimicrob. Agents Chemother. **42:**1437–1446.
6. **Cherniak, R., and J. B. Sundstrom.** 1994. Polysaccharide antigens of the capsule of *Cryptococcus neoformans*. Infect. Immun. **62:**1507–1512.
7. **Cherniak, R., H. Valafar, L. C. Morris, and F. Valafar.** 1998. *Cryptococcus neoformans* chemotyping by quantitative analysis of ^{1}H nuclear magnetic resonance spectra of glucuronoxylomannans with a computer-simulated artificial neural network. Clin. Diagn. Lab. Immunol. **5:**146–159.
8. **Cherniak, R., L. C. Morris, B. C. Anderson, and S. A. Meyer.** 1991. Facilitated isolation, purification, and analysis of glucuronoxylomannan of *Cryptococcus neoformans*. Infect. Immun. **59:**59–64.
9. **Datta, K., and L. A. Pirofski.** 2006. Towards a vaccine for *Cryptococcus neoformans*: principles and caveats. FEMS Yeast Res. **6:**525–536.
10. **Dische, Z.** 1947. A specific color reaction for glucuronic acid. J. Biol. Chem. **171:**725–730.
11. **Dromer, F., J. Charreire, A. Contrepois, C. Carbon, and P. Yeni.** 1987. Protection of mice against experimental cryptococcosis by anti-*Cryptococcus neoformans* monoclonal antibody. Infect. Immun. **55:**749–752.
12. **Dromer, F., J. Salamero, A. Contrepois, C. Carbon, and P. Yeni.** 1987.

Production, characterization, and antibody specificity of a mouse monoclonal antibody reactive with *Cryptococcus neoformans* capsular polysaccharide. Infect. Immun. **55:**742–748.
13. **Dubois, M., K. Gilles, J. K. Hamilton, P. A. Rebers, and F. Smith.** 1951. A colorimetric method for the determination of sugars. Nature **168:**167.
14. **Dykstra, M. A., L. Friedman, and J. W. Murphy.** 1977. Capsule size of *Cryptococcus neoformans*: control and relationship to virulence. Infect. Immun. **16:**129–135.
15. **Farhi, F., G. S. Bulmer, and J. R. Tacker.** 1970. *Cryptococcus neoformans*. IV. The not-so-encapsulated yeast. Infect. Immun. **1:**526–531.
16. **Feitosa, M. I., and O. N. Mesquita.** 1991. Wall-drag effect on diffusion of colloidal particles near surfaces: a photon correlation study. Phys. Rev. A **44:**6677–6685.
17. **Garcia-Hermoso, D., F. Dromer, and G. Janbon.** 2004. *Cryptococcus neoformans* capsule structure evolution in vitro and during murine infection. Infect. Immun. **72:**3359–3365.
18. **Gates, M. A., P. Thorkildson, and T. R. Kozel.** 2004. Molecular architecture of the *Cryptococcus neoformans* capsule. Mol. Microbiol. **52:**13–24.
19. **Granger, D. L., J. R. Perfect, and D. T. Durack.** 1985. Virulence of *Cryptococcus neoformans*. Regulation of capsule synthesis by carbon dioxide. J. Clin. Investig. **76:**508–516.
20. **Jacobson, E. S., M. J. Tingler, and P. L. Quynn.** 1989. Effect of hypertonic solutes upon the polysaccharide capsule in *Cryptococcus neoformans*. Mycoses **32:**14–23.
21. **Janbon, G.** 2004. *Cryptococcus neoformans* capsule biosynthesis and regulation. FEMS Yeast Res. **4:**765–771.
22. **Jung, W. H., A. Sham, R. White, and J. W. Kronstad.** 2006. Iron regulation of the major virulence factors in the AIDS-associated pathogen *Cryptococcus neoformans*. PLoS Biol. **4:**e410.
23. **Kamerling, J. P., G. J. Gerwig, J. F. Vliegenthart, and J. R. Clamp.** 1975. Characterization by gas-liquid chromatography-mass spectrometry and proton-magnetic-resonance spectroscopy of pertrimethylsilyl methyl glycosides obtained in the methanolysis of glycoproteins and glycopeptides. Biochem. J. **151:**491–495.
24. **Kozel, T. R.** 1995. Virulence factors of Cryptococcus neoformans. Trends Microbiol. **3:**295–299.
25. **Kozel, T. R., S. M. Levitz, F. Dromer, M. A. Gates, P. Thorkildson, and G. Janbon.** 2003. Antigenic and biological characteristics of mutant strains of *Cryptococcus neoformans* lacking capsular O acetylation or xylosyl side chains. Infect. Immun. **71:**2868–2875.
26. **Larsen, R. A., P. G. Pappas, J. Perfect, J. A. Aberg, A. Casadevall, G. A. Cloud, R. James, S. Filler, and W. E. Dismukes.** 2005. Phase I evaluation of the safety and pharmacokinetics of murine-derived anticryptococcal antibody 18B7 in subjects with treated cryptococcal meningitis. Antimicrob. Agents Chemother. **49:**952–958.
27. **Maxson, M. E., E. Dadachova, A. Casadevall, and O. Zaragoza.** 2007. Radial mass density, charge, and epitope distribution in the *Cryptococcus neoformans* capsule. Eukaryot. Cell **6:**95–109.
28. **McFadden, D., O. Zaragoza, and A. Casadevall.** 2006. The capsular dynamics of *Cryptococcus neoformans*. Trends Microbiol. **14:**497–505.
29. **McFadden, D. C., M. De Jesus, and A. Casadevall.** 2006. The physical properties of the capsular polysaccharides from *Cryptococcus neoformans* suggest features for capsule construction. J. Biol. Chem. **281:**1868–1875.
30. **Monari, C., F. Bistoni, and A. Vecchiarelli.** 2006. Glucuronoxylomannan exhibits potent immunosuppressive properties. FEMS Yeast Res. **6:**537–542.
31. **Mukherjee, J., G. Nussbaum, M. D. Scharff, and A. Casadevall.** 1995. Protective and nonprotective monoclonal antibodies to *Cryptococcus neoformans* originating from one B cell. J. Exp. Med. **181:**405–409.
32. **Mukherjee, J., M. D. Scharff, and A. Casadevall.** 1992. Protective murine monoclonal antibodies to *Cryptococcus neoformans*. Infect. Immun. **60:**4534–4541.
33. **Nakouzi, A., P. Valadon, J. D. Nosanchuk, N. Green, and A. Casadevall.** 2001. Molecular basis for immunoglobulin M specificity to epitopes in *Cryptococcus neoformans* polysaccharide that elicit protective and nonprotective antibodies. Infect. Immun. **69:**3398–3409.
34. **Perfect, J. R., and A. Casadevall.** 2002. Cryptococcosis. Infect. Dis. Clin. N. Am. **16:**837–874.
35. **Pericolini, E., E. Cenci, C. Monari, M. De Jesus, F. Bistoni, A. Casadevall, and A. Vecchiarelli.** 2006. *Cryptococcus neoformans* capsular polysaccharide component galactoxylomannan induces apoptosis of human T-cells through activation of caspase-8. Cell. Microbiol. **8:**267–275.
36. **Rivera, J., M. Feldmesser, M. Cammer, and A. Casadevall.** 1998. Organ-dependent variation of capsule thickness in *Cryptococcus neoformans* during experimental murine infection. Infect. Immun. **66:**5027–5030.
37. **Rodrigues, M. L., L. Nimrichter, D. O. Oliveira, S. Frases, K. Miranda, O. Zaragoza, M. Alvarez, A. Nakouzi, M. Feldmesser, and A. Casadevall.** 2007. Vesicular polysaccharide export in *Cryptococcus neoformans* is a eukaryotic solution to the problem of fungal trans-cell wall transport. Eukaryot. Cell **6:**48–59.
38. **Taylor, R. L., and H. E. Conrad.** 1972. Stoichiometric depolymerization of polyuronides and glycosaminoglycuronans to monosaccharides following reduction of their carbodiimide-activated carboxyl groups. Biochemistry **11:**1383–1388.
39. **Tripp, C., A. Ruiz, and G. S. Bulmer.** 1981. Culture of Cryptococcus neoformans in the nonencapsulated state. Mycopathologia **76:**129–131.
40. **Viana, N. B., M. S. Rocha, O. N. Mesquita, A. Mazolli, P. A. Maia Neto, and H. M. Nussenzveig.** 2006. Absolute calibration of optical tweezers. Appl. Phys. Lett. **88:**131110.
41. **Viana, N. B., M. S. Rocha, O. N. Mesquita, A. Mazolli, P. A. Maia Neto, and H. M. Nussenzveig.** 2007. Towards absolute calibration of optical tweezers. Phys. Rev. **75:**021914.
42. **Vincken, J. P., H. A. Schols, R. J. Oomen, M. C. McCann, P. Ulvskov, A. G. Voragen, and R. G. Visser.** 2003. If homogalacturonan were a side chain of rhamnogalacturonan I. Implications for cell wall architecture. Plant Physiol. **132:**1781–1789.
43. **Yoneda, A., and T. L. Doering.** 2006. A eukaryotic capsular polysaccharide is synthesized intracellularly and secreted via exocytosis. Mol. Biol. Cell. **17:**5131–5140.
44. **Zaragoza, O., A. Telzak, R. A. Bryan, E. Dadachova, and A. Casadevall.** 2006. The polysaccharide capsule of the pathogenic fungus *Cryptococcus neoformans* enlarges by distal growth and is rearranged during budding. Mol. Microbiol. **59:**67–83.
45. **Zaragoza, O., B. C. Fries, and A. Casadevall.** 2003. Induction of capsule growth in *Cryptococcus neoformans* by mammalian serum and CO_2. Infect. Immun. **71:**6155–6164.
46. **Zimm, B. H.** 1948. The scattering of light and the radial distribution function of high polymer solutions. J. Chem. Phys. **16:**1093–1099.